Coherent A_1 phonons in Te studied with tailored femtosecond pulses

2007 J. Phys.: Condens. Matter 19 406220

(http://iopscience.iop.org/0953-8984/19/40/406220)

IOP PUBLISHING JOURNAL OF PHYSICS: CONDENSED MATTER

J. Phys.: Condens. Matter **19** (2007) 406220 (12pp) doi:10.1088/0953-8984/19/40/406220

Coherent A_1 phonons in Te studied with tailored femtosecond pulses

O V Misochko[1], M V Lebedev[1], H Schäfer[2] and T Dekorsy[2]

[1] Institute of Solid State Physics, Russian Academy of Sciences, 142432 Chernogolovka, Moscow region, Russia
[2] Physics Department, Konstanz University, 78457 Konstanz, Germany

E-mail: misochko@issp.ac.ru

Received 12 July 2007, in final form 24 August 2007
Published 12 September 2007
Online at stacks.iop.org/JPhysCM/19/406220

Abstract

We tailor the shape and phase of the pump-pulse spectrum in order to study coherent lattice dynamics in tellurium. Employing coherent control by splitting the pump pulse into a two-pulse sequence, we show that the oscillations due to A_1 coherent phonons can be cancelled but not enhanced as compared to single-pulse excitation of the same energy. We further demonstrate that a crucial factor for coherent phonon generation seems to be the bandwidth of the pulse spectrum. We observe that the coherent amplitude for long pump pulses decreases exponentially with pulse duration for both Gaussian and rectangular pulses. Finally, by varying the pulse chirp, we show that the coherent amplitude is independent of the chirp sign while the oscillation lifetime is slightly dependent on the chirp sign.

(Some figures in this article are in colour only in the electronic version)

1. Introduction

Soon after the first observation of coherent phonons (i.e. lattice vibrations where all atoms move in phase with each other) in semimetals and narrow band semiconductors [1], Zeiger *et al* suggested a cogent explanation for the creation of lattice coherence in opaque materials called displacive excitation of coherent phonons (DECP) [2]. In this mechanism, following an ultrafast optical excitation, a significant fraction of the valence electrons is excited to higher electronic states. Such step-like excitation greatly reduces the attractive part of the interatomic potential and allows the atoms to move with their thermal velocities towards a new equilibrium state. Some time later, it was suggested [3, 4] that DECP is a particular (resonance) case of impulsive stimulated Raman scattering (ISRS), a mechanism which had been suggested earlier to explain the coherent vibrations of molecules and atoms in transparent crystals [5, 6]. ISRS relies exclusively on the spectral bandwidth of an ultrashort pulse [5–9] which exceeds the phonon frequency, thus allowing the pulse to exert a temporally impulsive driving force on

the atoms. Such a force gives momentum to the atoms, changing their thermal velocities. Since the lattice interacts with light only through electrons, both mechanisms rely on the specific (deformation potential) electron–phonon coupling, leaving electron–photon interaction to a great extent unspecified. Taking a simple analogy with a classical pendulum, one can relate non-resonant ISRS to kicking the pendulum (i.e. applying a real force) and thereby to changing its kinetic energy, whereas DECP can be related to modifying the potential energy of the pendulum (i.e. applying an imaginary force). The main difference between the two models is the role of the electromagnetic field in the creation of the lattice coherence [7, 9]. In DECP, any macroscopic variable affected by the optic field and coupled to the lattice can be used as the driving force provided that the variable can be switched in a time shorter than the phonon period. In this case, the light penetration depth defines both the phonon amplitude and wavevector, while the energy is supplied to the lattice through a linear intensity absorption process. In resonant ISRS, where the energy is supplied to the lattice by a Stokes process, the electromagnetic field defines not only the phonon amplitude and wavevector (through the kinematic selection rules), but also the phonon symmetry (through the symmetry selection rules). Thus, the differences between resonant ISRS and DECP include the possibility for the former to coherently excite non-symmetric phonons and the requirement of phase matching based on kinematic constraints during the generation process [7].

Although there are the numerous theoretical models for describing the lattice coherence [6, 7, 10, 11], each theory ultimately describes the phonon's coherent amplitude Q as a driven harmonic oscillator:

$$\frac{\mathrm{d}^2 Q}{\mathrm{d}t^2} + \alpha \frac{\mathrm{d}Q}{\mathrm{d}t} + \Omega^2 Q = F(t),$$

where Ω is the phonon frequency, α is the damping parameter and F is the driving force. The coherent amplitude Q is further related to the experimentally observed oscillatory amplitude of transient reflectivity. However, the questions—what is coherence and how coherent are the coherent phonons?—are still far from being resolved. For example, there are conflicting answers to the first question for opaque crystals: Kurz and co-workers suggested [10] that the coherence in the phonon subsystem is caused by synchronized motion of different wavevector phonons whose phases are locked, while Kuznetsov and Stanton ascribed the coherence to the result of simultaneously occurring multiphonon processes within a single phonon mode [11]. The first model relies on a continuous spectrum, and the lattice state can be understood within a classical framework, while the second (quantum-mechanical) model describes the coherent state as a Glauber state. Unfortunately, neither of the models specifies how to quantitatively measure the lattice coherence despite the fact that the coherence is a measurable quantity. Therefore in this work we will simply trace the behaviour of the oscillatory amplitude of transient reflectivity as a function of the laser pulse parameters, leaving aside the question how exactly the amplitude is connected to the lattice coherence.

In this paper, the goal is to study the role of the electromagnetic field in the coherent phonon generation process. Since ultrashort laser pulses intrinsically consist of a broad range of frequency components, this provides the possibility of modifying the pulse spectrum through a controlled change of the amplitude and phase for each frequency. Such femtosecond pulse shaping has opened up a wide range of intriguing possibilities for controlling and manipulating lattice dynamics. The objective of studies in optical control over coherent phonons is to prepare a crystal in a non-equilibrium state in order to influence, and therefore to study, its evolution on femtosecond time scales. Pioneering experiments on lattice coherent control were performed in organic [12] and transparent crystals [13], and similar, though much simpler, studies have been conducted for opaque crystals at low [14, 15] and high [16–19] excitation strength. The lattice coherent control is possible in the pump–probe experiments owing to a stable phase

of the lattice oscillations, which allows the oscillations to be switched on and off according to a specific control parameter (in our case chosen to be the interpulse separation). We will use the pulse shaping and coherent control techniques to clarify the role of photons in the generation of lattice coherence. A favourable candidate to investigate the photon contribution in the creation of lattice coherence should be a simple crystal, which is relatively easy to handle, both theoretically and experimentally. For that reason, in our study single crystal tellurium is used as a benchmark system as it has been extensively studied in the time domain [1, 2, 20–26].

2. Experimental details

The crystal structure D_3^4 of tellurium consists of three-atoms-per turn helices whose axes are arranged on a hexagonal lattice. Among six optical phonons, the fully symmetric A_1 phonon (frequency $\Omega \approx 3.6$ THz) is a lattice mode for which the helical radius changes, leaving the interhelical distance and c-axis spacing unchanged. Although all optical phonons in Te have been excited coherently [20, 22], the A_1 phonon mode is usually dominant as a result of a large deformation potential for the symmetry preserving movements [26]. To further eliminate any contribution of unwanted optical phonons, we excite the coherent phonons in our study with a pump polarized along the trigonal axis, thus avoiding the generation of coherent phonons of lower symmetry [22, 25]. Note that such geometry allows exciting coherent phonons through a change in the extraordinary part of the susceptibility χ_{ext}, while the probing process is based on the optical response through a change in the ordinary part of the susceptibility χ_{ord}. Before describing our experimental results, we would like to stress that the task of settling the question as to which of the excitation mechanisms is the dominant one (or what is their interrelation) cannot be answered ultimately on the basis of our experiments. The theoretical calculations in [2, 21] support the DECP picture with respect to the fully symmetric A_1 mode in Te, but the Raman framework or other mechanism based, for example, on the ultrafast photo-Dember field effect [23] are definitely required to account for the excitation of non-symmetry preserving or non-Raman active coherent phonons.

Our laser system is based on a conventional Ti:sapphire laser which supplies 50 fs–800 nm pulses with a repetition rate of 82 MHz. Part of the beam was used as the pump pulse. The remaining part was used as the probe pulse, which is always a unchirped, transform-limited pulse. The pump pulse was tailored with a pulse shaper comprising a spatial light modulator utilizing liquid crystals [27]. This approach to ultrafast pulse shaping involves a spatial Fourier transformation of the incident pulse to disperse the frequencies in space and modify the chosen frequency components selectively. A final recombination of all the frequencies into a single collimated beam results in the desired pulse shape. In our set up, a 1200 groves mm^{-1} grating spreads the pulse, so that each different spectral component maps onto a different spatial position. The collimating cylindrical lenses and grating pair are set up in a modified 4f stretcher configuration (f being the focal length of the lenses) with three lenses instead of one for two reasons. First, we are able to shorten the distance between the gratings to nearly 2f, thus reducing the influence of acoustic noise. Second, we obtain a better focus in the plane of the liquid crystals by taking the beam divergence into account. The liquid crystal double mask (Jenopik GmbH), consisting of 320 stripes, is placed so that it modulates the spectrum. Both the tailored pump and the transform-limited probe were focused by a single 10 cm lens onto the sample. At the sample surface they were linearly (orthogonal to each other) polarized in the plane of incidence. The transient reflectivity was measured with a fast scanning delay line. A polarizer was inserted between the sample and the p–i–n detector to prevent scattered pump light from reaching the detector and to ensure that only properly polarized light is measured. To establish time zero, the roles of the pump and probe were reversed and the zero delay time

was precisely determined by locating the point of mirror symmetry. The error in establishing time zero was less than 5 fs. The pulse duration of the probe was measured with a standard autocorrelator to get transform-limited pulses at the output. A cross-correlation between pump and probe was used to calibrate the pulse shaper phase modulation, concerning the chirp of additional glass in the pump line. The cross-correlation of the tailored pump pulse with the bandwidth-limited probe pulse was taken each time to confirm the correct modulation.

3. Experimental results and discussion

Given that tellurium at room temperature is a narrow band semiconductor, after the ultrafast excitation at $\lambda = 800$ nm (1.55 eV), both coherent phonons and free carriers are excited simultaneously [1, 2]. As a result the fast oscillations in transient reflectivity are observed superimposed onto the electronic decay with picosecond decay time. To separate the oscillatory $(\frac{\Delta R}{R_0})_{\rm osc}$ and electronic $(\frac{\Delta R}{R_0})_{\rm el}$ contributions, we will usually fit the signal to a convolution $\frac{\Delta R}{R_0} \propto \int_0^t A(\tau)H(t-\tau)\,{\rm d}\tau$ of the expected delta-function response

$$H(x) = \left[\left(\frac{\Delta R}{R_0}\right)_{\rm el} \exp(-x/\tau_{\rm el}) + \left(\frac{\Delta R}{R_0}\right)_{\rm osc} \exp(-x/\tau_{\rm osc})\sin(\Omega x + \varphi)\right]$$

with the pulse shape $A(\tau)$, where Ω and $\tau_{\rm osc}$ are the frequency and lifetime of oscillations, while $\tau_{\rm el}$ is the electronic relaxation time. As expected, the oscillation parameters obtained from the time-domain analysis are nearly the same as those obtained from the frequency domain fits performed by the use of time-integrated fast Fourier transform.

We first split the 50 fs transform-limited pulse into two identical Gaussian pulses with a different interpulse separation γ. Figure 1(a) shows the transient reflectivity of Te excited with such two-pulse sequence (each pulse is unchirped). The four traces in the figure illustrate the changes in the response when the interpulse separation γ is varied. The traces from the bottom to the top correspond to an interpulse separation γ of 80, 140, 200, and 280 fs, respectively. If the total electronic contribution is always the sum of the signals resulting from each pulse independently, the oscillatory component exhibits interferences resulting in a variation of the total amplitude as a function of γ. As shown in figure 1(b), depending on the interpulse separation, the oscillatory component can be almost completely cancelled but not enhanced as compared to single-pulse excitation (that is $(\frac{\Delta R}{R_0})_{\rm osc}^{\gamma=0} \geqslant (\frac{\Delta R}{R_0})_{\rm osc}^{\gamma\neq 0}$). On the other hand, a time delay of $\gamma = nT$ between the two pump pulses, where n is an integer and $T = \Omega^{-1}$ is the phonon period, results in an enhancement while a time delay of $(n + 1/2)T$ results in cancellation of the oscillations created by the first pulse, i.e. cancellation or enhancement is sensitive to the arrival time of the second pump pulse relative to the first, as expected. That is, the coherent oscillations created by the *first* pulse can be either cancelled or enhanced. The latter option is realized with the restriction that the resulting amplitude cannot be larger than that created by the single pulse of the same energy as the two-pulse sequence. Thus, splitting the excitation energy (or the number of photons) between multiple pulses provides selectivity, but not increase in the resulting coherent amplitude, suggesting that the lattice excitation is proportional to the total energy (or intensity) of the laser pulse.

In contrast to the high excitation density case [16–18], our experiments show that the oscillations under low excitation densities can be cancelled *exactly* at the maximum displacement when the coherent amplitude has the opposite sign compared to that at time zero. Indeed, the 140 fs pulse separation that achieves almost full cancellation as shown in figure 1(a) coincides with the time to reach the maximum displacement (inner classical turning point) in the single-pulse pump case, since the oscillation period is approximately 280 fs and the

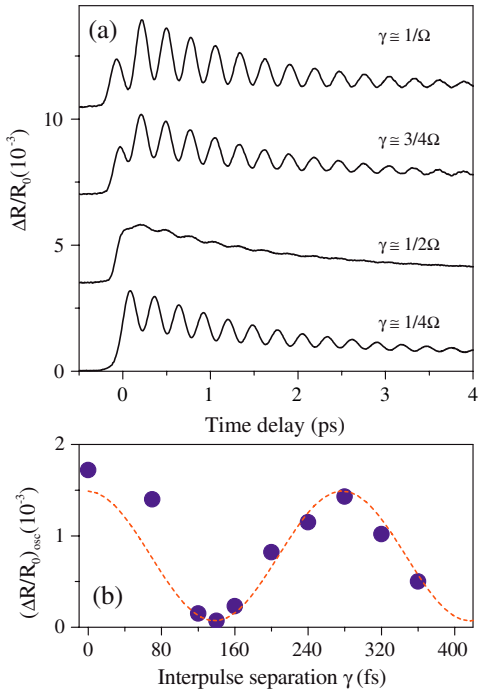

Figure 1. Differential reflectivity in Te versus time delay for two-pulse excitation (a). The average incident power of the pump pulses is 50 mW. The interpulse separation γ is indicated for each trace displaced vertically for clarity. (b) Coherent amplitude as a function of the interpulse separation γ.

oscillation starts at the outer turning point[3]. Similar cancellation of coherent vibrations at the maximum displacement has been observed in bismuth [15] and GaAs [14] for weak excitation densities.

In the low excitation regime, interaction between an ultrashort pulse and a crystal can be explained adequately by perturbation theory. For one-photon transitions, this means that the interaction varies linearly with the exciting field. Thus, the crystal response to a two-pulse sequence can be described either by summing the contributions of each pulse, or by considering directly the effect of the total exciting field. Although not correct in general, in our case the coherent control can be well understood as the sum of two sets of coherent phonons whose motion is initiated at different times and that then interfere (this description ignores the interaction of the second pulse with already excited coherent movement). This model was first introduced in [15] to describe the coherent control of A_{1g} phonons in Bi at low excitation strengths. Nevertheless, what we observe is not the simple sum of two single-pulse signals $R_1^{t=0}(t) + R_2^{t=\gamma}(t)$ with γ being the control parameter, but the transient reflectivity change $\chi_{\rm tot}(t)$ that is set-up by the sum of two oscillating susceptibilities $\chi_1^{t=0}(t) + \chi_2^{t=\gamma}(t)$. Only because our square root detectors measure essentially $|\chi_{\rm tot}(t)|^2$ in which cross-terms with oscillatory components vanish, we cannot see the difference between $R_1^{t=0}(t) + R_2^{t=\gamma}(t)$ and $\chi_1^{t=0}(t) + \chi_2^{t=\gamma}(t)$.

[3] In tellurium, density functional theory calculations [21] show that transferring electrons from the valence band to the conduction band changes the potential surface so that a larger equilibrium helical radius is established. Nevertheless, experimental studies disagree on this point, suggesting either expansion [17] or contraction [24] of the helical radius after the photoexcitation.

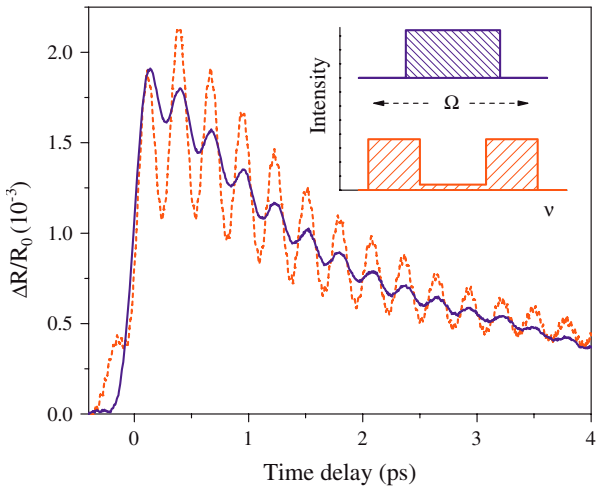

Figure 2. Differential reflectivity in Te versus time delay for the pump pulses with rectangular spectra. Their spectra (offset for clarity) are schematically shown in the inset. The dashed (red) trace and the solid (blue) trace correspond to the pump pulses whose bandwidths are correspondingly smaller or larger than the phonon frequency.

Given that in Te the non-equilibrium carrier distribution drives coherent phonons, the process of coherent control can be better thought of in the following way [17]: the first pump pulse creates a new potential in which the atoms will move. Initially displaced from the newly established equilibrium configuration, the lattice reaches this configuration in approximately one quarter of a phonon period, but due to inertia the atoms have momentum at that point and continue to move. When the atoms reach the classical turning point (located on the opposite slope of the potential) of their motion, a second pump pulse can excite the precise density of carriers to shift the equilibrium position to the current position of the atoms, stopping the oscillatory motion. Because the photoexcitation of additional carriers can only increase (or decrease) the equilibrium helical radius (see footnote 3), the vibration can only be stopped at the maximum displacement (when atoms are located on the opposite slope of the potential as compared to that from where the movement starts) as is observed in our experiments.

A second set of experiments focuses on the question as to what is more important for coherent phonon generation: the pulse spectrum or the steepness of the leading edge of the pulse envelope? To separate these two effects, we used pulses with different, almost rectangular, spectra that form a kind of sinc-function in the time domain. Coherent oscillations for two different spectra of the pump pulse were studied: the rectangular spectrum with bandwidth smaller than the phonon frequency, and the spectrum with a hole in the middle (in this case the overall bandwidth is larger than the phonon frequency) and figure 2 shows the oscillations excited by such tailored pulses. As expected, a relatively large oscillatory amplitude is observed for the case with the pulse spectrum containing the phonon frequency. In contrast, the oscillations almost disappear (their amplitudes are approximately five times smaller) when the spectrum is narrower than the phonon frequency. Note that the electronic contributions $(\frac{\Delta R}{R_0})_{\rm el}^{\rm max}$ in both cases almost coincide and the different oscillatory amplitude cannot be *quantitatively* explained by the constructive interference resulting from the two-pulse sequence in the case of the spectrum with a hole (even if the nT criterion for enhancement is satisfied it cannot result in fivefold enhancement). The vanishing oscillatory amplitude $(\frac{\Delta R}{R_0})_{\rm osc}$ in the case of a

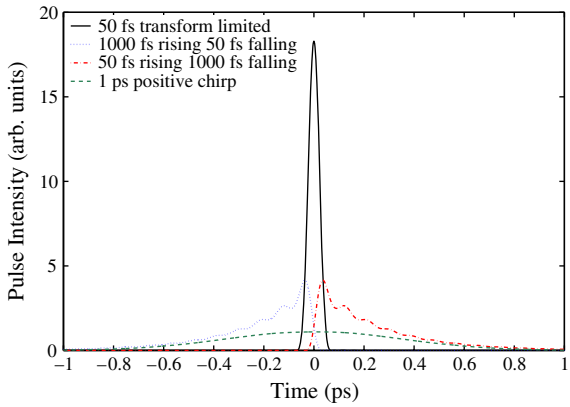

Figure 3. Temporal profiles of the sawtooth pulses. For a comparison purpose, temporal profiles of the 50 fs transform-limited pulse and of the 1 ps positively chirped pulse of the same energy are also shown.

single sinc-pulse challenges to some extent the applicability of DECP as the primary excitation mechanism for fully symmetric phonons. Indeed, in the DECP picture, a crucial requirement for coherent phonon generation, is that the changes induced by the exciting pulse are abrupt, that is the driving force is step-like. The abruptness can be related to a steepness of the leading edge of the pulse envelope. Therefore, approximating the sinc-pulse by a triangular function in the time domain

$$I(t) = \Delta\left(\frac{t}{\tau}\right) = \begin{cases} 1 - \dfrac{|t|}{\tau} & \text{if } -\frac{1}{2}\tau < t \leqslant \frac{1}{2}\tau \\ 0 & \text{otherwise} \end{cases}$$

one can see that the pulse with a broader spectrum has a steeper leading edge than each of the two triangular pulses formed from the spectrum with a hole in the middle because the bandwidth of each pulse is narrower than that of the single (broader spectrum) pulse[4]. Thus, this observation seems to suggest that a crucial condition to effectively create the lattice coherence is the bandwidth of the pulse spectrum. Such a condition implies that the pump process can be somehow related to biharmonic pumping (either two photon absorption, or scattering) that involves at least two field–matter interactions necessary for the energy transfer and the coherence creation.

In order to further clarify the role of the pulse envelope, we compare coherent phonons excited with sawtooth pulses (i.e. pulses having a linear rise on the leading edge and a virtually instantaneous fall on the trailing edge, or conversely, a virtually instantaneous rise and a linear fall). These two types of sawtooth pulse are shown in figure 3 together with a 50 fs transform limited and a 1 ps positively chirped pulse. These pulse shapes are ideally suited to study the effects of the leading edge since their temporal profiles are inverted in time. In addition, their spectra (almost identical) were chosen to be significantly narrow than the phonon frequency, see figure 4. Unexpectedly, coherent oscillations $(\frac{\Delta R}{R_0})_{\text{osc}}$ excited with such sawtooth pulses are almost equal, with relatively large oscillatory amplitude, reaching one half of that observed for the 50 fs transform-limited pump pulse of the same energy, see figure 5. The comparable oscillatory amplitudes indicate that coherent phonon generation seems to be independent of the

[4] Note, however, that the spectral components of the two spectral parts separated by the hole might interfere and therefore cause a steep component in the time domain.

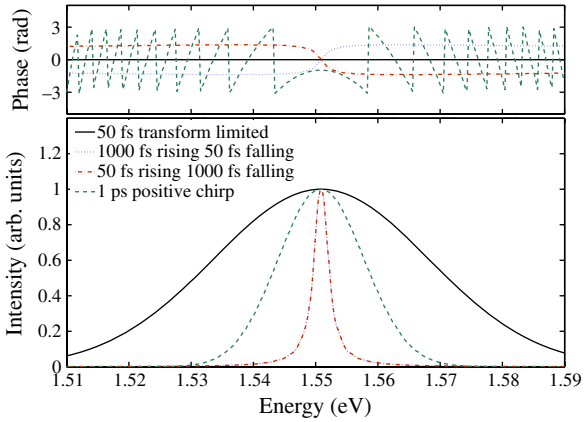

Figure 4. Calculated spectra of the pulses shown in figure 3, the spectra of the different sawtooth pulses overlap.

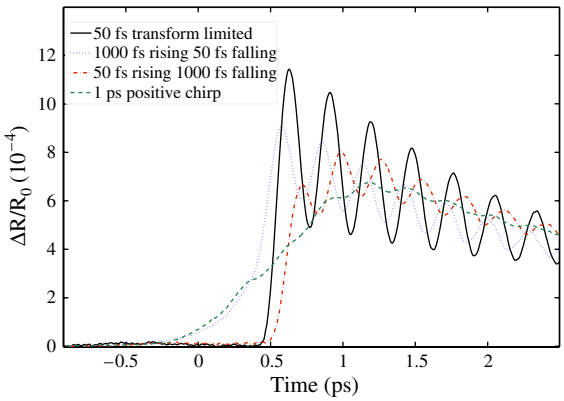

Figure 5. Differential reflectivity versus time delay for the pulses shown in figure 3. The zero delay point is not calibrated.

steepness of the leading edge. However, the result for the sawtooth pulses is, at first glance, in conflict with that obtained for the sinc-pulses since the spectral bandwidth of the used sawtooth pulses is much smaller than the phonon frequency. One way of resolving the discrepancy between the sinc and sawtooth pulses is to assume that the coherent oscillations observed with sawtooth pulses are due the spectral sidebands intrinsic for the pulses of such a temporal profile. Indeed, a closer inspection of the temporal profile reveals that a linear rise (drop) in both cases is slightly modulated with the ≈80 fs period, multiples of which are comparable with the inverse of the phonon frequency. In this case the number and the temporal separation of the subpeaks, which coincide for both types of the used sawtooth pulses, can essentially define the resulting amplitude.

Following coherent control experiments, we next focus our attention on the question: how does the duration of a single laser pulse affect the creation of lattice coherence? Even though it is well known that the pulse duration has to be shorter than the phonon period (or equivalently the spectral width of the pump pulse has to be broader than the phonon frequency) in order to achieve efficient coherent excitation, the experimental demonstration of this requirement

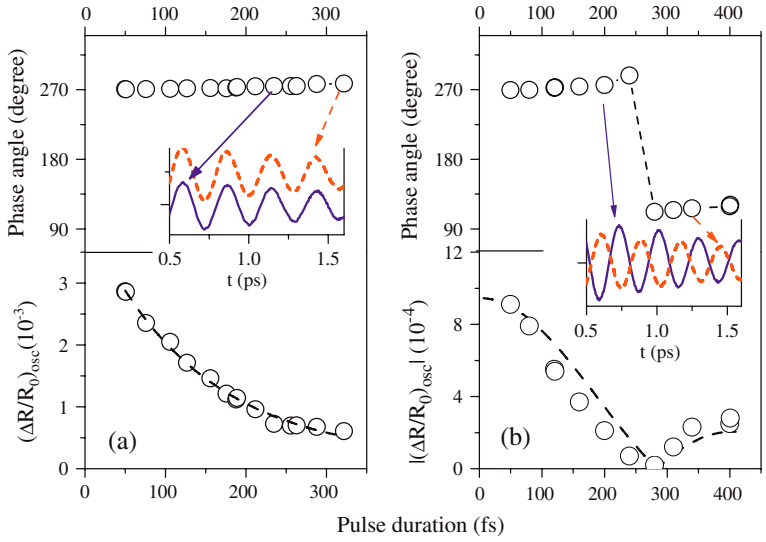

Figure 6. Amplitude and phase of the coherent A_1 oscillations as a function of the pulse duration for Gaussian (a) and rectangular (b) pulses. Dashed lines are fits using exponential and sinc functions, respectively. The insets show the oscillatory part at chosen time delays for the pulses with duration shorter (blue, solid line) and longer (red, dashed line) than the phonon period. In the left inset the traces are offset for clarity.

has not yet been realized, at least for opaque materials. In order to study the effect of the pulse duration, we generate Gaussian and rectangular pulses of different bandwidths and trace the parameters of the transient response as a function of the pulse duration which is inversely proportional to the bandwidth. Figure 6 reflects the influence of the pulse stretching on the efficiency of lattice excitation for the two different spectral line shapes. For a Gaussian pulse, the coherent amplitude $(\frac{\Delta R}{R_0})_{\rm osc}$ decreases exponentially with pulse duration, see figure 6(a). The characteristic pulse duration for the amplitude reduction is 75 fs $\approx T/4$ as obtained from the fit to an exponential function. There is a simple physical reason behind this relation, which can be explained by the model of a driven pendulum with a period of $T = \Omega^{-1}$ and which is initially in its equilibrium position. An external perturbation, in our case linked to the electromagnetic field, can accelerate it most effectively in the first quarter of its period, i.e. $\tau = T/4$. If the perturbation is shorter or longer than $T/4$, the pendulum will not receive the optimal energy and its amplitude will decrease [28].

For a Gaussian pulse, we identify no detectable phase lag of the oscillations, most probably due to the fact that damping is significantly smaller than any of the pulse durations. In contrast, for a rectangular pulse

$$I(t) = \mathrm{rect}\left(\frac{t}{\tau}\right) = \begin{cases} 1 & \text{if } -\frac{1}{2}\tau < t \leqslant \frac{1}{2}\tau \\ 0 & \text{otherwise} \end{cases}$$

the modulus of oscillatory amplitude $|(\frac{\Delta R}{R_0})_{\rm osc}|$ is not a smooth function of the pulse duration. It follows the regular sinc-function $(=\frac{\sin \Omega\tau}{\Omega\tau})$ dependence, changing the sign at $\tau = \frac{1}{\Omega}$, with Ω being the phonon frequency. When the pulse duration matches the phonon period the amplitude changes its sign. This means that the phase experiences a π jump at this duration as observed in our experiments and shown in the inset of figure 6(b).

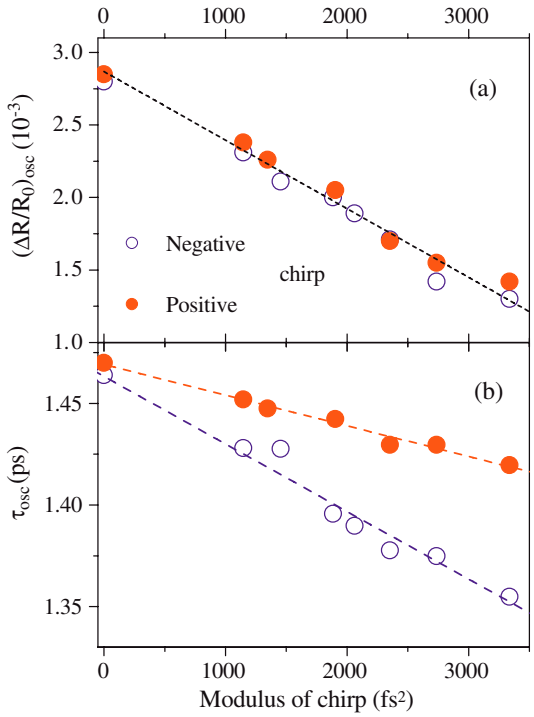

Figure 7. Chirp dependence of the coherent amplitude (a), and of the oscillation lifetime (b). Open (blue) and closed (red) symbols are for negatively and positively chirped pulses, respectively. Dashed lines are linear fits.

It is interesting to note that the electronic contribution $(\frac{\Delta R}{R_0})_{el}$ is independent of pulse duration as could also be inferred from the coherent control experiments. Since in our experiments the stretching of the pulses is achieved under the condition that the energy of the pulse is approximately conserved (as the mask covers a broader part of the spectrum of the initial transform-limited pulse, the pulse becomes less stretched and its intensity increases) we conclude that the coherent amplitude is proportional to pulse intensity, whereas the non-equilibrium carrier concentration is proportional to pulse energy. In other words, long and short pulses of equal energy excite the same density of electrons, leading to the same displaced equilibrium position, but long pulses excite a smaller amplitude coherent phonon than short pulses.

In our previous experiments the chirp was set to zero, i.e. only the amplitude but not the phase of the electromagnetic field was modulated. Finally, we study experimentally the influence of a linear chirp on the coherent phonon generation process. In this last set of experiments, we vary not only the magnitude, but also the direction of the chirp. By using either positively (blue follows red) or negatively (red follows blue) chirped pulses, the arrival time of each frequency component at the crystal can be controlled. For a larger absolute value of linear chirp and therefore for longer pulse durations, the electronic contribution $(\frac{\Delta R}{R_0})_{el}$ and oscillation frequency Ω remain essentially unchanged. On the other hand, the larger the chirp, the smaller is the oscillation amplitude. More exactly, the oscillatory contribution $(\frac{\Delta R}{R_0})_{osc}$, shown in figure 7, continuously disappears for a larger chirp with a rate that is independent of the chirp sign. By comparing this decrease with the changes observed for unchirped pulses

of different bandwidth, we conclude that this reduction is trivial being simply due to a larger duration of the chirped pulses. Note that the observed insensitivity to the chirp sign at low excitation strength is in striking contrast to the case of amplified pulses where strong asymmetry for positively and negatively chirped pulses has been observed recently [25]. Nevertheless, the lifetimes of the oscillations do show a small asymmetry in the dependence on the chirp sign, indicating that the oscillations created with positively chirped pulses live longer than those generated with negatively chirped ones. Given that the same durations for positively and negatively chirped pulses yield the asymmetry of lifetimes, such behaviour cannot be explained by the temporal broadening only. Relying on a similar observation for coherent vibrational excitation in molecules [29], we tentatively ascribe this asymmetry to different contributions of the ground and excited electronic states involved in the creation of the lattice coherence. These different contributions may be due to the fact that by tailoring the spectral phase of the pulse, we control the interference between the various spectral components, leading to a selective population of given phonon energy levels.

4. Conclusions

In summary, our experiments are the first demonstration of a pulse-shaping strategy where a complex shape (in phase and amplitude) has been applied to study the coherent lattice dynamics in a simple opaque crystal. The experiments have demonstrated that in Te a necessary condition for the effective excitation of coherent A_1 phonons is the bandwidth of the pump pulse. This fact suggests that both linear and nonlinear interactions between the pump and the crystal are important. By coherent control experiments, we have proven that coherent amplitude can be cancelled but not enhanced if the excitation energy is split into two pulses. At the low excitation strength used in our study the oscillations are stopped exactly at the maximum displacement, corresponding to the inner turning point or time delays of $n + 1/2$ phonon periods between successive pump pulses. Next, we have shown that an increase in the pulse duration results in an exponential decrease of the coherent amplitude, independent of the pulse envelope. However, it turns out that for the pulses with a rectangular envelope, the modulus of amplitude is not a smooth function and the phase of coherent phonons experiences a π-phase jump when the pulse duration matches the phonon period. In addition, we observe that long and short pulses of equal energy excite the same density of electrons, leading to the same displaced equilibrium position. However, long pulses excite smaller amplitude coherent phonons than short pulses. Finally, varying chirp and its sign, we have established that for low excitation strength the chirp sign does not affect the oscillation amplitude but brings on a small asymmetry in the dependence of oscillation lifetime on the chirp sign. We hope that the results obtained reveal a wealth of information needed for a better understanding of coherent lattice dynamics of opaque crystals and for the construction of a future quantitative theory.

Acknowledgments

This work was supported in part by the Deutsche Forschungsgemeinschaft (DE567/9) and by the Russian Foundation for Basic Research (06-02-16186 and 07-02-00148).

References

[1] Cheng T K, Vidal J, Zeiger H J, Dresselhaus G, Dresselhaus M S and Ippen E P 1991 *Appl. Phys. Lett.* **59** 1923
[2] Zeiger H J, Vidal J, Cheng T K, Ippen E P, Dresselhaus G and Dresselhaus M S 1992 *Phys. Rev.* B **45** 768
[3] Garrett G A, Albrecht T F, Whitaker J F and Merlin R 1996 *Phys. Rev. Lett.* **77** 3661

[4] Stevens T E, Kuhl J and Merlin R 2002 *Phys. Rev.* B **65** 144304
[5] Chesnoy J and Mokhtari A 1988 *Phys. Rev.* A **38** 3566
[6] For a review, see e.g. Dhar L, Rogers J A and Nelson K A 1994 *Chem. Rev.* **94** 167
[7] Merlin R 1997 *Solid State Commun.* **102** 207
[8] Dekorsy T, Cho G C and Kurz H 2000 *Light Scattering in Solids VIII* ed M Cardona and G Güntherodt (Berlin: Springer) p 169
[9] Misochko O V 2001 *Zh. Eksp. Teor. Fiz.* **119** 285
Misochko O V 2001 *J. Exp. Theor. Phys.* **92** 246 (Engl. Transl.)
[10] Pfeifer T, Kütt W, Kurz H and Scholz R 1992 *Phys. Rev. Lett.* **69** 3248
[11] Kuznetsov A V and Stanton C J 1994 *Phys. Rev. Lett.* **73** 3243
[12] Weiner A M, Leaird D E, Wiederrecht G P and Nelson K A 1990 *Science* **247** 1317
[13] Wefers M M, Kawashima H and Nelson K A 1996 *J. Phys. Chem. Solids* **57** 1425
[14] Dekorsy T, Kutt W, Pfeifer T and Kurz H 1993 *Europhys. Lett.* **23** 223
[15] Hase M, Mizoguchi K, Harima H, Nakashima S, Tani M, Sakai K and Hangyo M 1996 *Appl. Phys. Lett.* **69** 2474
[16] DeCamp M F, Reis D A, Bucksbaum P H and Merlin R 2001 *Phys. Rev.* B **64** 092301
[17] Roeser C A D, Kandyla M, Mendioroz A and Mazur E 2004 *Phys. Rev.* B **70** 212302
[18] Murray E D, Fritz D M, Wahlstrand J K, Fahy S and Reis D A 2005 *Phys. Rev.* B **72** 060301(R)
[19] Misochko O V, Lu R, Hase M and Kitajima M 2007 *Zh. Eksp. Teor. Fiz.* **131** 275
Misochko O V, Lu R, Hase M and Kitajima M 2007 *J. Exp. Theor. Phys.* **104** 245 (Engl. Transl.)
[20] Hunsche S, Wienecke K, Dekorsy T and Kurz H 1995 *Phys. Rev. Lett.* **75** 1815
[21] Tangney P and Fahy S 2002 *Phys. Rev.* B **65** 054302
[22] Misochko O V, Lebedev M V and Dekorsy T 2005 *J. Phys.: Condens. Matter* **17** 3015
[23] Dekorsy T, Auer H, Bakker H J, Roskos H G and Kurz H 1996 *Phys. Rev.* B **53** 4005
[24] Hunsche S, Wienecke K and Kurz H 1996 *Appl. Phys.* A **62** 502
[25] Misochko O V, Dekorsy T, Andreev S V, Kompanets V O, Matveets Yu A, Stepanov A G and Chekalin S V 2007 *Appl. Phys. Lett.* **90** 071901
[26] Kudryashov S I, Kandyla M, Roeser C A D and Mazur E 2007 *Phys. Rev.* B **75** 08520
[27] Lee K G, Kim D S, Yee K J and Lee H S 2006 *Phys. Rev.* B **74** 113201
[28] Zhang G P and George T F 2004 *Phys. Rev. Lett.* **93** 147401
[29] Bardeen C J, Wang Q and Shank C V 1995 *Phys. Rev. Lett.* **75** 3410